JACS
JOURNAL OF THE AMERICAN CHEMICAL SOCIETY

COMMUNICATION

pubs.acs.org/JACS

Photochemically and Electrochemically Triggered Au Nanoparticles "Sponges"

Dora Balogh, Ran Tel-Vered, Ronit Freeman, and Itamar Willner*

The Center for Nanoscience and Nanotechnology and the Institute of Chemistry, The Hebrew University of Jerusalem, Jerusalem 91904, Israel

Supporting Information

ABSTRACT: Stimuli-triggered wettability of surfaces and controlled uptake and release of substrates by "smart" materials are essential for drug delivery and microfluidic control. A composite "sponge" consisting of bis-aniline-bridged Au nanoparticles (NPs), functionalized with photoisomerizable nitrospiropyran/nitromerocyanine that includes selective imprinted molecular recognition sites for *N*,*N*′-bis(3-sulfonatopropyl)-4,4′-bipyridinium (PVS) was electropolymerized on a Au electrode. The system is triggered by photonic and/or electrical signals to yield four different states exhibiting variable binding/release capacities for PVS and controlled wettability of the surface. The electrical/optical uptake and release of PVS to and from the Au NPs "sponge", respectively, is followed by CdSe/ZnS quantum dots, acting as an auxiliary photonic label.

Control of the wettability of surfaces has attracted substantial research efforts[1−4] directed toward the development of self-cleaning materials,[5] the dictated transport of fluids,[6] and the prevention of biofouling[7] or corrosion.[8] Different external triggers, such as thermal,[9,10] electrical,[11−13] optical,[14−16] or chemical[17,18] stimuli, were used to reversibly switch the wetting properties of surfaces modified with electroactive, photoactive, or pH-sensitive monolayers or functionalized with thermosensitive, photoactive, or electroactive thin polymer films. The tailoring of signal-triggered micro-/nanocontainer systems has also evoked extensive research efforts aimed toward the development of switchable, controlled uptake and release systems. For example, the phototriggered release of substrates from mesoporous materials[19] and the pH-stimulated dissociation of supramolecular complexes[20] represent stimuli-controlled release from organized nanostructures. Here we report on the construction of a photochemically and electrochemically triggered Au nanoparticles (NPs) composite "sponge" on a surface. We demonstrate the light/electrical-controlled uptake and release of a substrate to and from the composite and reveal that the wettability of the surface is controlled by these external triggers. Furthermore, since the matrix is activated by two inputs (electrical and optical) that generate four distinct interconvertable states, one may consider the system as a four-state automaton.

We have recently introduced a method to imprint molecular recognition sites in cross-linked Au NPs composites synthesized on conductive surfaces.[21−23] Specifically, we demonstrated that the electropolymerization of thioaniline-functionalized Au NPs on thioaniline-functionalized Au surfaces, in the presence of molecular templates that yield π-donor−acceptor or electrostatic complexes with the thioaniline units, led to the formation of bis-aniline-cross-linked Au NPs composites that encapsulated the template molecules in the matrices.[21] Subsequent rinsing-off of the template molecules yielded molecular imprinted sites with high affinity for the association of the imprinting templates or their structural analogues. For example, using picric acid or Kemp's acid as imprinting templates, imprinted matrices for the selective and ultrasensitive detection of trinitrotoluene (TNT)[21] or trinitrotriazine (RDX)[22] were developed, respectively. Similarly, the redox activity of the bis-aniline bridges cross-linking the Au NPs was implemented to develop imprinted Au NPs composites for the selective electrochemical uptake and release of substrates.[24] For example, by imprinting molecular recognition sites for the *N*,*N*′-dimethyl-4,4′-bipyridinium (MV^{2+}) electron acceptor in the Au NPs composite, electroswitchable, reversible uptake and release of MV^{2+} to and from the imprinted sites was accomplished. In this system, MV^{2+} was associated to the imprinted sites via π-donor−acceptor interactions with the bis-aniline bridging units, whereas electrochemical oxidation of the bridges to the respective quinoid state, exhibiting acceptor features, released the MV^{2+} molecules from the matrix. Similarly, the electrochemical uptake and release of the MV^{2+} guest substrate to and from the imprinted Au NPs composite was found to control the wettability of the surface.[25] While the association of the charged MV^{2+} to the imprinted sites enhanced the hydrophilicity of the surface, the release of the electron acceptor from the composite made the surface less hydrophilic.

The synthesis of an imprinted Au NPs composite, acting as an opto-electrical "sponge" for the controlled uptake and release of a substrate by photonic or electrochemical stimuli, is depicted in Figure 1. Au nanoparticles (3.5 nm) were functionalized with a mixed monolayer consisting of thioaniline (**1**), *N*-mercaptobutyl nitrospiropyran (**2a**), and mercaptoethyl sulfonic acid (**3**). The photoisomerizable nitrospiropyran component, **2a**, was photoconverted to the zwitterionic merocyanine isomer state, **2b** (λ = 365 nm; Figure 1a). The resulting Au NPs interacted with the zwitterionic electron acceptor, *N*,*N*′-bis(3-sulfonatopropyl)-4,4′-bipyridinium (PVS, **4**), and were electropolymerized on a thioaniline-functionalized Au surface in the presence of **4** as the imprinting template (Figure 1b). The template molecules **4** interact with the Au NPs by π-donor−acceptor interactions with the thioaniline donor sites and by electrostatic interactions between their zwitterionic parts and the zwitterionic merocyanine photoisomer. The imprinting template was then washed off of the bis-

Received: February 1, 2011
Published: April 11, 2011

dx.doi.org/10.1021/ja2009899 | *J. Am. Chem. Soc.* 2011, 133, 6533–6536

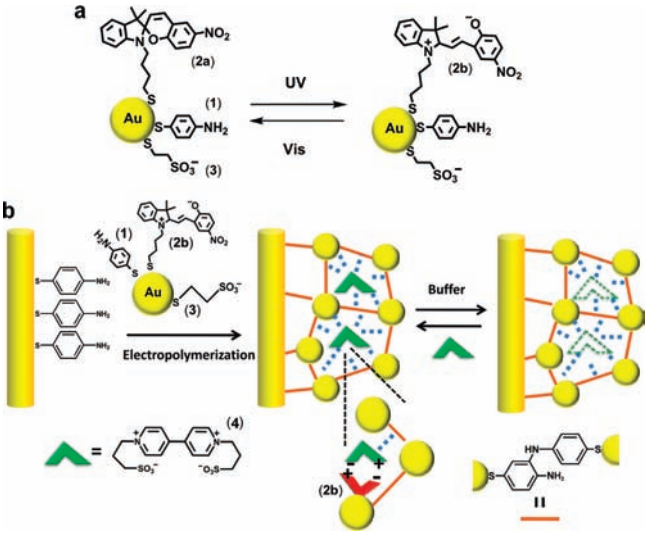

Figure 1. (a) Reversible photochemical isomerization of the nitrospiropyran (**2a**)-modified Au NPs to the merocyanine (**2b**) photoisomer by UV irradiation (λ = 365 nm), and back to **2a** by irradiation with visible light (λ > 495 nm). The Au NPs are capped with a mixed monolayer of thioaniline (**1**), mercaptobutyl nitrospiropyran (**2a**), and mercaptoethyl sulfonic acid (**3**). (b) Schematic presentation of the electropolymerization of the bis-aniline-cross-linked Au NPs composite and the imprinting of the zwitterionic electron acceptor, *N*,*N*′-bis(3-sulfonatopropyl)-4,4′-bipyridinium (PVS, **4**), into the composite.

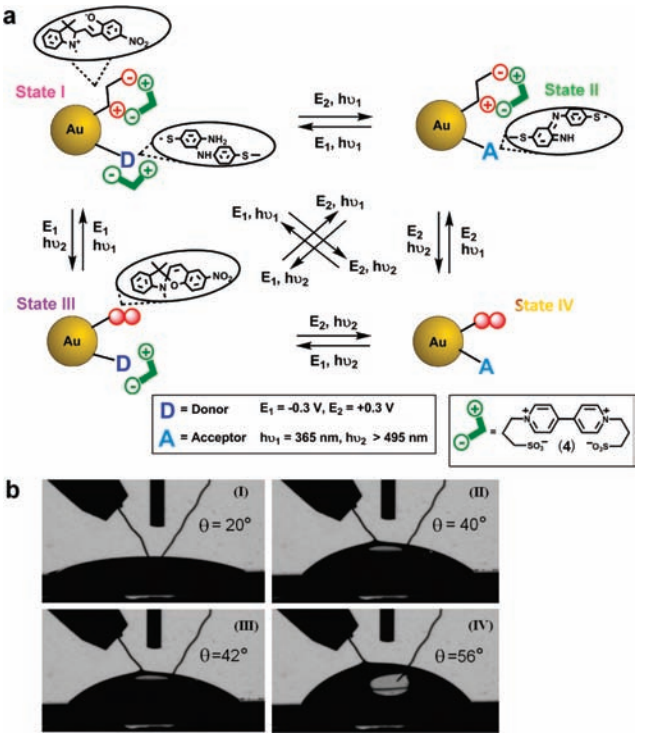

Figure 2. (a) Optical/electrochemical transitions between the four possible states of the bis-aniline-cross-linked **2a**/**2b**-modified Au NPs composite and the respective association of PVS to the different states. (b) Images showing changes in the contact angle, θ, for a droplet containing 200 mM PVS on the PVS-imprinted bis-aniline-cross-linked Au NPs electrode upon the application of four different triggers on the electrode for the generation of four different states: (I) E = −0.3 V vs Ag QRE and λ = 365 nm; (II) E = +0.3 V and λ = 365 nm; (III) E = −0.3 V and λ > 495 nm; (IV) E = +0.3 V and λ > 495 nm.

aniline-cross-linked Au NPs composite to yield the PVS-imprinted matrix. By a similar procedure, merocyanine/thioaniline-functionalized Au NPs were electropolymerized on a thioaniline monolayer-modified Au surface, in the absence of PVS, to yield the non-imprinted composite. The bis-aniline bridging units exhibit a quasi-reversible redox wave at $E^{\circ\prime}$ = 0.32 V vs SCE, at pH 7.4. The nitro groups of the nitrospiropyran units are irreversibly reduced to the hydroxylamine state. These properties enabled us to estimate the average coverage of the matrix with the bis-aniline units to be 1.1×10^{14} units·cm^{-2} and with nitrospiropyran to be 8.2×10^{-11} mol·cm^{-2}. Coverage of the surface by the Au NPs was estimated by quartz crystal microbalance to be 4.0×10^{12} NPs·cm^{-2} (for details on the characterization of the surface, see the Supporting Information (SI)). A ±5% reproducibility in the composite formation was observed in a set of N = 6 experiments.

The imprinted matrix may exist in four different states that exhibit variable affinities for the zwitterionic electron acceptor **4**, hence resulting in different wettability features of the surface (Figure 2a). In state I, the bridging units exist in the donor bis-aniline configuration, while the photoisomerizable units exist in the zwitterionic structure. Under these conditions, the electron acceptor PVS binds to the two components by both donor−acceptor and electrostatic interactions, giving rise to a surface exhibiting the highest hydrophilicity. Electrochemical oxidation of the bis-aniline bridges to the quinoid units, state II, prohibits the binding of PVS to the bridging units by donor−acceptor interactions, while retaining the electrostatic interactions with the merocyanine groups. This leads to a surface with intermediate hydrophilicity. Photochemical isomerization (λ > 495 nm) of the merocyanine units of the Au NPs in state I to the nitrospiropyran (**2a**) configuration yields state III, where the cross-linking bridges exist in the bis-aniline donor structure, while the photoactive units are present in the noncharged nitrospiropyran isomer state. In state III, the PVS binds to the functionalized NPs only by donor−acceptor interactions, giving rise to intermediate hydrophilicity of the surface. Electrochemical oxidation of the bis-aniline bridges cross-linking the Au NPs in state III to the quinoid structure yields state IV, where both the electroactive bridges (acceptors) and the photoactive components (nitrospiropyran) lack binding affinity for PVS. This yields the state with the lowest hydrophilicity (enhanced hydrophobicity). The different states of the Au NPs composites can also be generated by other pathways. For example, state IV can be generated directly from state I by the application of an oxidative trigger, E = +0.3 V vs Ag wire (Ag QRE), and a photochemical input, λ > 495 nm.

Figure 2b depicts the images and contact-angle values of an aqueous droplet that includes 200 mM PVS upon interaction with the different states of the PVS-imprinted Au NPs composite. When the Au NPs composite exists in state I, the water droplet exhibits a flat shape, demonstrating a contact angle of θ = 20°, which implies a very hydrophilic surface, consistent with the effective association of PVS to the matrix. In contrast, in state IV, where PVS interacts poorly with the composite, the droplet is repelled by the matrix, leading to a surface of enhanced hydrophobicity, θ = 56°. In states II and III, partial association of PVS to the composite occurs, leading to an intermediate hydrophilicity, as reflected by contact angle values of θ = 40° and 42°, respectively.

Photo-/electrochemical control of the wettability of the surface is reversible upon the application of the respective external triggers.

dx.doi.org/10.1021/ja2009899 |*J. Am. Chem. Soc.* 2011, 133, 6533–6536

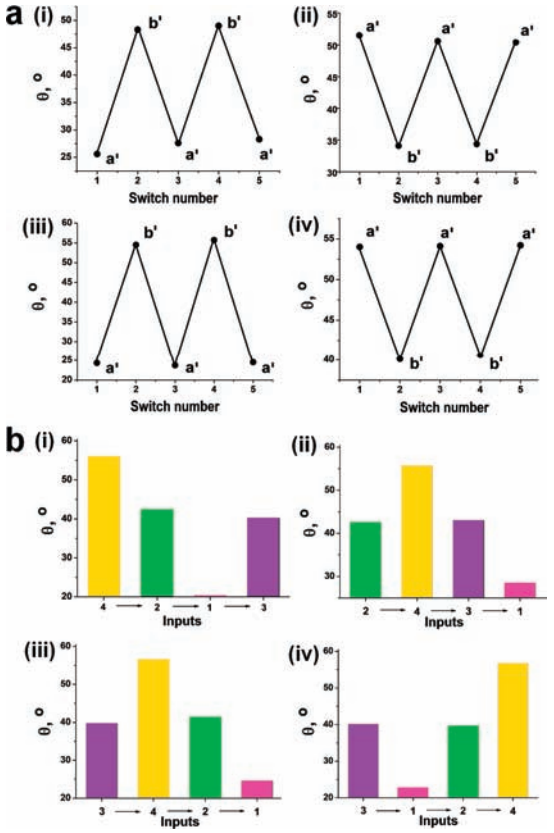

Figure 3. (a) Cyclic switching of the contact angle of an aqueous droplet containing 200 mM PVS on a PVS-imprinted bis-aniline-cross-linked Au NPs electrode upon the application of (i) photochemical pulses [(a′) λ = 365 nm and (b′) λ > 495 nm], (ii) electrochemical pulses [(a′) E = 0.3 V and (b′) E = −0.3 V], (iii) combined photochemical and electrochemical triggers [(a′) λ = 365 nm and E = −0.3 V (input 1) and (b′) λ > 495 nm and E = 0.3 V (input 4)], and (iv) combined photochemical and electrochemical triggers [(a′) λ > 495 nm and E = 0.3 V and (b′) λ > 495 nm and E = 0.3 V (input 3)]. (b) Contact angle values for the droplet in (a) upon the application of the four different combinations of electrochemical and optical triggers in different orders: (i) 4 → 2 → 1 → 3; (ii) 2 → 4 → 3 → 1; (iii) 3 → 4 → 2 → 1; (iv) 3 → 1 → 2 → 4. Input 2 corresponds to λ = 365 nm and E = 0.3 V.

For example, Figure 3a-i shows the photostimulated cycling of the wettability properties of the composite upon photoisomerization of the nitrospiropyran units to the zwitterionic configuration and back, while the cross-linking bridging units are in the bis-aniline state. Evidently, the contact angles are cycled between low and high values, respectively. Similarly, Figure 3a-ii shows the cyclic electrochemical control of the wettability of the surface for a case where the Au NPs are functionalized by the nitrospiropyran photoisomer and the bis-aniline bridges are reversibly oxidized and reduced to the quinoid and bis-aniline states, respectively. Parts iii and iv of Figure 3a correspond to the reversible electro-/photochemical cycling of states I ⇌ IV and states IV ⇌ III, respectively, (For the reversible cycling of the wettability properties of the surface upon cycling the system between the other pairs of states, states IV ⇌ II, states I ⇌ II, and states III ⇌ I, see SI Figure S3.)

Furthermore, one may cycle the system from any state to all other states by application of the appropriate optical/electrical signals. Figure 3b-i exemplifies the stepwise transitions across the different states, where the initial configuration of the system is fixed at state IV (which includes the bridges in the oxidized quinoid form and the photoactive components in the nitrospiropyran isomer state). This composite does not bind PVS, which results in the high contact angle value. Reduction of the bridges to the bis-aniline state yields state II, which corresponds to intermediate hydrophilicity. Furthermore, photoisomerization of the nitrospiropyran to the merocyanine photoisomer generates state I, having higher binding affinity for PVS, and this results in the composite of highest hydrophilicity (θ = 20°). Finally, state I is converted to state III by oxidation of the bis-aniline units to the quinoid state. This leads to the association of PVS only to the zwitterionic merocyanine isomer, giving rise to a surface of intermediate hydrophilicity (θ = 40°). Similarly, parts ii, iii, and iv of Figure 3b depict the sequential transitions between states II → IV → III → I, states III → IV → II → I, and states III → I → II → IV, respectively. (For the cyclic activation of the system between states III → II → IV → I, see SI Figure S4-i.)

Several control experiments that demonstrate the significance of the imprinting process for generating the effective photonic/electrochemical "sponge", and which also reveal selective control of the wettability, were performed: (i) The non-imprinted composite consisting of the bis-aniline-cross-linked Au NPs modified with the photoisomerizable units shows only minute contact angle changes upon interaction with PVS. (see SI Figure S4-ii). These results indicate that PVS exhibits low affinity for association to the non-imprinted matrix, leading to the very small changes in the contact angle values. Indeed, complementary chronocoulometric experiments that followed the charge associated with the reduction of PVS on the PVS-imprinted matrix (in state I) versus the non-imprinted matrix enabled us to evaluate the association constant of PVS to the imprinted sites, $K_a^{IM} = 6.4 \times 10^4\ M^{-1}$, and to compare it to the weaker affinity of PVS to the non-imprinted composite, $K_a^{NI} = 8 \times 10^3\ M^{-1}$ (see SI Figure S5). The higher association constant of PVS to the imprinted composite facilitates the significant contact angle changes observed upon the application of optical/electrical triggers. (ii) The effect of the interaction of *N*,*N*′-dimethyl-4,4′-bipyridinium (MV^{2+}, **5**) with the PVS-imprinted composite, subjected to the different optical/electrical signals, was similarly examined (see SI Figure S4-iii). We find that the interaction of MV^{2+} with the PVS-imprinted matrix has only minute effects on the contact angle values of the droplet subjected to the different states of the composite. These results indicate that the imprinted sites are specific for PVS and that the structurally related electron acceptor **5** reveals poor affinity for the PVS-imprinted sites.

Finally, the quantitative uptake and release of PVS to and from the different states of the composite were evaluated. Toward this goal, the Au NPs composite-modified electrode was introduced into a solution of PVS, and following the optical/electrical triggered uptake/release of PVS to/from the composite, the solution was interacted with CdSe/ZnS quantum dots as auxiliary optical labels (the QDs were capped with the zwitterionic glutathione **6**, Figure 4a). Using the fact that PVS quenches the luminescence of the modified QDs, and extracting the appropriate calibration curve (see SI Figure S6), the concentration of PVS in the solution could be determined for each state of the composite. In state IV, where neither the quinoid bridges nor the nitrospiropyran photoisomer units bind PVS, the quenching of the QDs is high, implying that the acceptor is concentrated in the solution [Figure 4b, curve (d)]. Photoisomerization of the nitrospiropyran units to the zwitterionic merocyanine groups and reduction of the bridges to the bis-aniline state results in state I, which exhibits the highest affinity for PVS. This is reflected by the high

dx.doi.org/10.1021/ja2009899 |*J. Am. Chem. Soc.* 2011, 133, 6533–6536

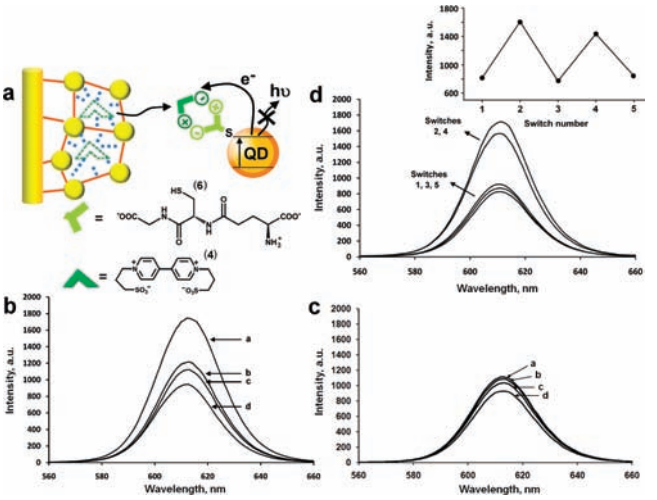

Figure 4. (a) Photonic imaging of the photochemical/electrochemical uptake and release of PVS to and from the PVS-imprinted bis-aniline-cross-linked Au NPs composite using CdSe/ZnS QDs as auxiliary optical labels. (b) Emission spectra corresponding to CdSe/ZnS quantum dots, 10^{-10} M in HEPES buffer solution (10 mM, pH 7.4), following their interaction for 20 min with a 200 pM PVS solution that was reacted with the PVS-imprinted Au NPs composite and upon the application of (curve a) $E = -0.3$ V vs Ag QRE and $\lambda = 365$ nm (state I), (curve b) $E = +0.3$ V and $\lambda = 365$ nm (state II), (curve c) $\lambda > 495$ nm and $E = -0.3$ V (state III), and (curve d) $\lambda > 495$ nm and $E = +0.3$ V (state IV) on the composite-modified electrode. (c) Same as in (b), for the non-imprinted Au NPs composite. (d) Emission spectra corresponding to the cyclic switching between states IV ⇌ I. Inset: The maximal fluorescence values, at $\lambda = 612$ nm, measured for the different states.

luminescence of the QDs that implies the uptake of PVS by the Au NPs matrix [Figure 4b, curve (a)]. From the luminescence changes of the QDs and the respective calibration curve, we estimate that ca. 1.8×10^{-13} mol·cm^{-2} of PVS were uptaken by the composite in state I. Upon conversion of the Au NPs composite into states II and III, the luminescence of the QDs reveals intermediate intensity values [Figure 4b, curves (b) and (c), respectively]. These luminescence values indicate that the uptake of PVS by the bis-aniline-bridged Au NPs composite in state II corresponds to 1.3×10^{-13} mol·cm^{-2}, whereas the uptake by the merocyanine groups in state III is 1.1×10^{-13} mol·cm^{-2}. Also, when the non-imprinted Au NPs composite was subjected to the different signals, generating states I–IV, only small luminescence changes of the QDs were observed (Figure 4c). This is consistent with the low binding capacity of PVS to the non-imprinted matrix. Furthermore, the reversible uptake and release of PVS to and from the imprinted composite were followed by the luminescence of the QDs. For example, Figure 4d shows the cyclic uptake and release of PVS upon transforming state IV to state I and back.

To conclude, the present study has introduced a new type of optoelectronic "sponge" consisting of imprinted Au NPs. The different states of the Au NPs composite generated surfaces of controlled wettabilities.

■ ASSOCIATED CONTENT

Ⓢ Supporting Information. Additional contact angle experiments performed on the composite-modified electrodes, coulometric analyses for the evaluation of the association constants, emission spectra for QDs interacted with variable concentrations of PVS, and synthesis of the PVS. This material is available free of charge via the Internet at http://pubs.acs.org.

■ AUTHOR INFORMATION

Corresponding Author
willnea@vms.huji.ac.il

■ ACKNOWLEDGMENT

This research is supported by NanoSensoMach ERC Grant No. 267574 under the EU FP7/2007-2013 program.

■ REFERENCES

(1) Zhang, X.; Shi, F.; Niu, J.; Jiang, Y. G.; Wang, Z. Q. *J. Mater. Chem.* **2008**, *18*, 621.
(2) Feng, X. J.; Jiang, L. *Adv. Mater.* **2006**, *18*, 3063.
(3) Sun, T. L.; Feng, L.; Gao, X. F.; Jiang, L. *Acc. Chem. Res.* **2005**, *38*, 644.
(4) Nath, N.; Chilkoti, A. *Adv. Mater.* **2002**, *14*, 1243.
(5) Wang, R.; Hashimoto, K.; Fujishima, A.; Chikuni, M.; Kojima, E.; Kitamura, A.; Shimohigoshi, M.; Watanabe, T. *Nature* **1997**, *388*, 431.
(6) Pollack, M. G.; Fair, R. B.; Shendrov, A. D. *Appl. Phys. Lett.* **2000**, *77*, 1725.
(7) Zhang, H.; Lamba, R.; Lewis, J. *Sci. Technol. Adv. Mater.* **2005**, *6*, 236.
(8) Liu, T.; Yin, Y. S.; Chen, S. G.; Chang, X. T.; Cheng, S. *Electrochim. Acta* **2007**, *52*, 3709.
(9) Sun, T. L.; Wang, G.; Feng, L.; Liu, B.; Ma, Y.; Jiang, L.; Zhu, D. *Angew. Chem. Int. Ed.* **2004**, *43*, 357.
(10) Huber, D. L.; Manginell, R. P.; Samara, M. A.; Kim, B. I.; Bunker, B. C. *Science* **2003**, *301*, 352.
(11) Riskin, M.; Basnar, B.; Chegel, V. I.; Katz, E.; Willner, I.; Shi, F.; Zhang, X. *J. Am. Chem. Soc.* **2006**, *128*, 1253.
(12) Abbott, N. L.; Gorman, C. B.; Whitesides, G. M. *Langmuir* **1995**, *11*, 16.
(13) Katz, E.; Lioubashevsky, O.; Willner, I. *J. Am. Chem. Soc.* **2004**, *126*, 15520.
(14) Oh, S. K.; Nakagawa, M.; Ichimura, K. *J. Mater. Chem.* **2002**, *12*, 2262.
(15) Vlassiouk, I.; Park, C. D.; Vail, S. A.; Gust, D.; Smirnov, S. *Nano Lett.* **2006**, *6*, 1013.
(16) Lahann, J.; Mitragotri, S.; Tran, T. N.; Kaido, H.; Sundaram, J.; Choi, I. S.; Hoffer, S.; Somorjai, G. A.; Langer, R. *Science* **2003**, *299*, 371.
(17) Kozlowskaya, V.; Kharlampieva, E.; Khanal, B. P.; Manna, P.; Zubarev, E. R.; Tsukruk, V. V. *Chem. Mater.* **2008**, *20*, 7474.
(18) Lee, D.; Nolte, A. J.; Kunz, A. L.; Rubner, M. F.; Cohen, R. E. *J. Am. Chem. Soc.* **2006**, *128*, 8521.
(19) Khashab, N. M.; Trabolsi, A.; Lau, Y. A.; Amborgio, M. W.; Friedman, D. C.; Khatib, H. A.; Zink, J. I.; Stoddart, F. *Eur. J. Org. Chem.* **2009**, *11*, 1169.
(20) Hernandez, R.; Tseng, H. R.; Wong, J. W.; Stoddart, J. F.; Zink, J. I. *J. Am. Chem. Soc.* **2004**, *126*, 3370.
(21) Riskin, M.; Tel-Vered, R.; Lioubashevski, O.; Willner, I. *J. Am. Chem. Soc.* **2009**, *131*, 7368.
(22) Riskin, M.; Tel-Vered, R.; Willner, I. *Adv. Mater.* **2010**, *22*, 1387.
(23) Ben-Amram, Y.; Riskin, M.; Willner, I. *Analyst* **2010**, *135*, 2952.
(24) Frasconi, M.; Tel-Vered, R.; Riskin, M.; Willner, I. *J. Am. Chem. Soc.* **2010**, *132*, 9373.
(25) Balogh, D.; Tel-Vered, R.; Riskin, M.; Willner, I. *ACS Nano* **2011**, *5*, 299.
(26) Willner, I.; Ford, W. E. *J. Heterocycl. Chem.* **1983**, *20*, 1113.